

## Near Infrared Optical Absorption of Gold Nanoparticle Aggregates

Thaddeus J. Norman, Jr., Christian D. Grant, Donny Magana, and Jin Z. Zhang\*

Department of Chemistry and Biochemistry, University of California, Santa Cruz, Santa Cruz, California 95064

Jun Liu

Sandia National Laboratories, Mail Stop 1413, P.O. Box 5800, Albuquerque, New Mexico 87185-1413

Daliang Cao and Frank Bridges

Department of Physics, University of California, Santa Cruz, Santa Cruz, California 95064

Anthony Van Buuren

Lawrence Livermore National Laboratory, 7000 East Avenue, Livermore, California 94550

Received: February 12, 2002; In Final Form: May 8, 2002

The reduction of  $\text{HAuCl}_4$  by  $\text{Na}_2\text{S}$  has been reported to produce gold nanoparticles with an optical absorption in the near-infrared along with its characteristic absorption in the visible. The optical resonances in the visible are due to the gold surface plasma, which are a function of the geometry of the particles. The near-infrared absorption had been attributed to the formation of  $\text{Au}_2\text{S}/\text{Au}$  core/shell structures. In this report we present new electronic absorption, electron microscopy, and X-ray absorption data in several systems to show that the near-infrared absorption does not involve core/shell structures. We further suggest that the near-infrared adsorption is most likely the result of the formation of aggregates of gold nanoparticles. The identification of the origin of the near-infrared resonance is critical in understanding the optical properties of metal nanoparticle systems.

### Introduction

Gold nanoparticles display optical properties that could potentially be exploited in optoelectronic devices.<sup>1</sup> The source of the optical absorption is the surface plasma resonance (SPR). For spherical gold particles the SPR occurs as a band centered at  $\sim 540$  nm. Small shifts in the position of the SPR occur as a result of changes in the dielectric properties of the medium the gold particles are in or the presence of materials adsorbed on the surface of the gold particle. Mie Scattering Theory is frequently used to explain the shifts in the SPR.<sup>2–4</sup> The theory predicts that shifts in the SPR can also occur when the particles deviate from spherical geometry. In this circumstance the transverse and longitudinal dipole polarizability no longer produce equivalent resonances. Consequently, two plasma resonances appear, a broadened and red shifted longitudinal plasma resonance, and a transverse plasma resonance, whose absorbance remains centered around 540 nm.<sup>4,5</sup>

Several colloidal gold systems, which typify this phenomenon, have been reported. They are gold nanorods,<sup>5–10</sup> gold aggregates,<sup>11–17</sup> and gold nanoshells.<sup>18–21</sup> The gold nanorods clearly display optical properties predicted by theory. As the aspect ratio increases, there is a red shift in the longitudinal plasma resonance while the position of the transverse resonance remains unchanged.<sup>9</sup> Gold aggregates show similar behavior. Aggregation causes a coupling of the gold nanoparticle's plasma modes, which results in a red shift and broadening of the longitudinal plasma resonance in the optical spectrum.<sup>11</sup> Gold shells have been grown on  $\text{SiO}_2$  nanoparticles and other colloidal material.<sup>21</sup>

When grown on  $\text{SiO}_2$ , the gold optical absorption shows distinct resonance for the transverse and longitudinal plasmon. The position and width of these resonances have been shown to be dependent upon the diameter of the  $\text{SiO}_2$  nanoparticle and the shell thickness.

Zhou et al. first reported that the reduction of  $\text{HAuCl}_4$  by  $\text{Na}_2\text{S}$  results in the formation of gold nanoshells on  $\text{Au}_2\text{S}$  nanoparticles.<sup>18</sup> The optical properties of this system were similar to that of the gold nanoshells grown on  $\text{SiO}_2$ .<sup>21</sup> As the reaction progressed, the two plasma resonances appear with one at  $\sim 530$  nm and another at  $\sim 630$  nm. They shifted during the reaction, and at times one appeared in the near-infrared region of the spectrum. The spectral evolution was shown to be dependent upon the ratio of  $\text{HAuCl}_4$  to  $\text{Na}_2\text{S}$  used and upon the method by which the  $\text{Na}_2\text{S}$  was added. From the TEM data it was concluded that gold had coated larger particles  $\text{Au}_2\text{S}$  particles. However, these data alone did not unambiguously demonstrate that gold nanoshells were forming on  $\text{Au}_2\text{S}$  nanoparticles.

Others have performed this experiment and have found no evidence for core–shell structures.<sup>22</sup> Following the same procedure a variety of particles of different morphology (rods, triangles, spheres, etc.) have been observed by TEM. The optical absorption does show the same trend in the time evolution that was observed by Zhou, but the time evolution of the spectrum was difficult to reproduce. Based on TEM data it was proposed that the shifting near-infrared absorbance observed by Zhou et al. was not due to the formation of gold nanoshells on  $\text{Au}_2\text{S}$  nanoparticles but to the formation of nonspherical gold nanoparticles.

\* Corresponding author.

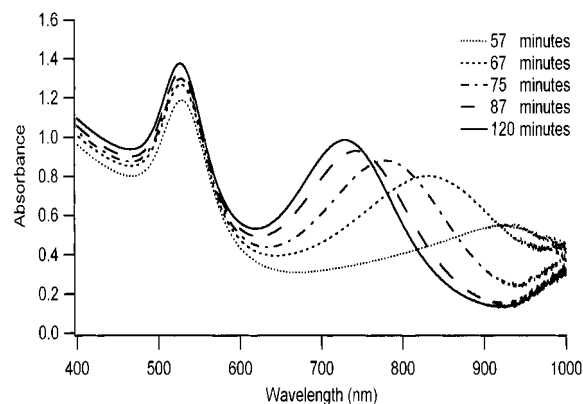


**Figure 1.** The evolution of the optical absorption spectrum following Method C. The second peak shifts from  $\sim 920$  to  $\sim 720$  nm while the first remains relatively constant at  $\sim 540$  nm.

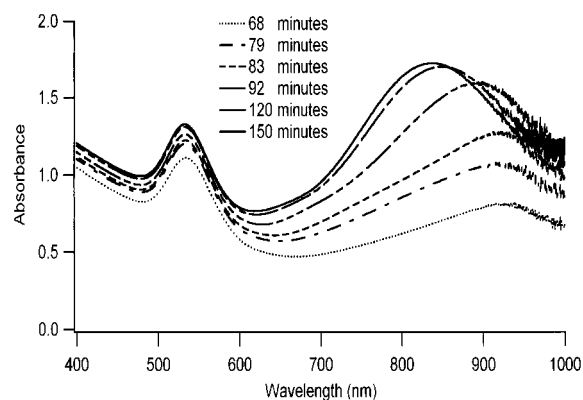


**Figure 2.** The evolution of the optical absorption spectrum following Method D. The second peak shifts from  $\sim 920$  to  $\sim 820$  nm while the first remains relatively constant at  $\sim 540$  nm.

Here, we present extensive experimental evidence to demonstrate that another, perhaps more likely, explanation for the observed near-IR absorption is that it is the result of the formation of aggregates of gold nanoparticles. In addition to performing the reduction of  $\text{HAuCl}_4$  by  $\text{Na}_2\text{S}$  using methods similar to Zhou et al., gold nanoparticle aggregates were synthesized by a different method without sulfur in order to exclude the effect of sulfur. The optical spectrums produced by the two methods were compared and found to be very similar. Also electron energy loss spectroscopy (EELS) measurements were taken in conjunction with high-resolution TEM to establish the size, composition, and morphology of the particles. These data suggest that the  $\text{HAuCl}_4$ - $\text{Na}_2\text{S}$  reaction produced gold aggregates. X-ray Absorption Fine Structure (XAFS) data taken on these samples at the Au  $L_3$  edge show no evidence of a distinct sulfur coordination shell and the unambiguous presence of metallic gold; yet, no sign of crystalline  $\text{Au}_2\text{S}_3$  was seen. From these results we propose that the reduction of  $\text{HAuCl}_4$  by  $\text{Na}_2\text{S}$  produces primarily aggregates of gold nanoparticles, and these aggregates are responsible for the observed near-IR resonance.

## Experiment

Gold nanoparticles were prepared by a variety of methods based on previous reported methods.<sup>18,23</sup>

**Method A.** A 100  $\mu\text{L}$  aliquot of a 0.1 M  $\text{Na}_2\text{S}$  solution was added to 40 mL of a  $5 \times 10^{-4}$  M  $\text{HAuCl}_4$  solution. The solutions were prepared with Milli-Q water and were stirred constantly. Five minutes after the addition of 100  $\mu\text{L}$   $\text{Na}_2\text{S}$  solution, another 20  $\mu\text{L}$  of 0.1 M  $\text{Na}_2\text{S}$  solution was added. Upon sulfide addition

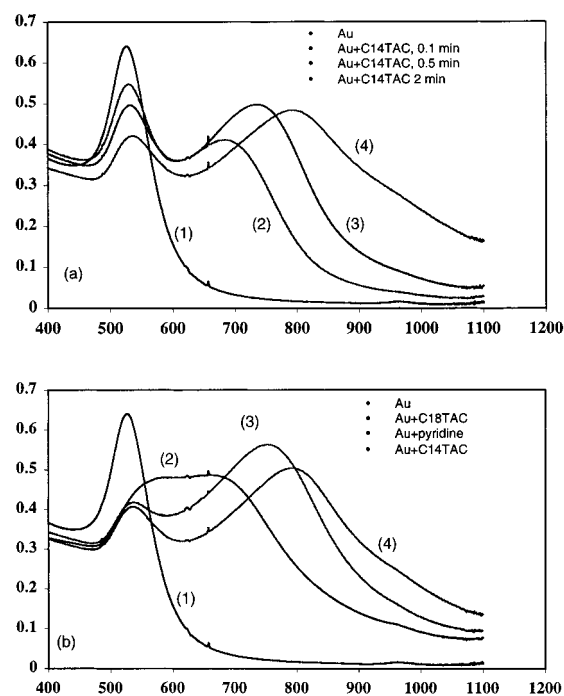


**Figure 3.** A) The UV spectra as a function of time when C14TAC is added. The second peak shifts from  $\sim 700$  to  $\sim 800$  nm with time, indicating a higher degree of aggregation. B) are the spectra with different additives. C14TAC is the surfactant with 14 carbon chains. C18TAC is the surfactant with 18 carbon chains.

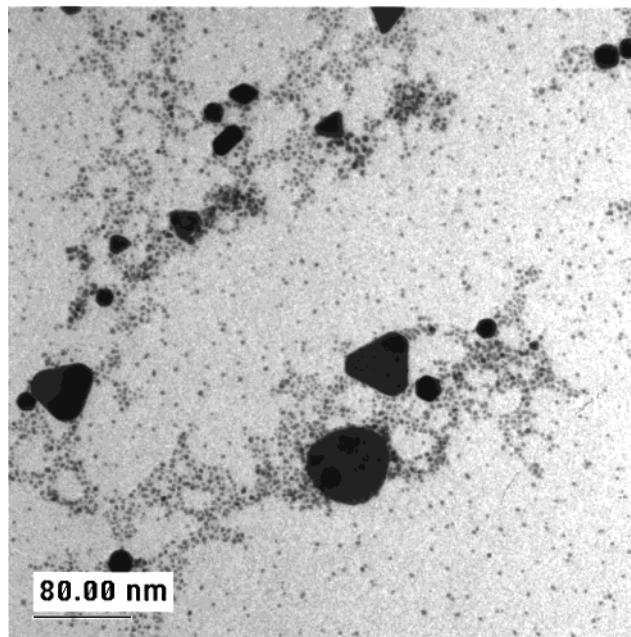


**Figure 4.** TEM micrograph of gold nanoparticles prepared by method C. The TEM sample was prepared 2 h after the reaction had begun.

the yellow  $\text{HAuCl}_4$  solution turned golden brown; however, after approximately 20 min the solution turned purple. As time progressed the solution retained its purple color but became progressively turbid. The pH of the  $\text{HAuCl}_4$  solution was 3 at the beginning of the reaction, but it dropped to 2.5 during the reaction. Within 48 h a reddish precipitate formed. The colloidal solution can be made stable for several months upon addition of PVA or PVP several minutes after sulfide addition. The absorption spectrum was taken regularly, using a Hitachi U-3000 and a HP 89532A spectrometer, to monitor the spectral evolution.

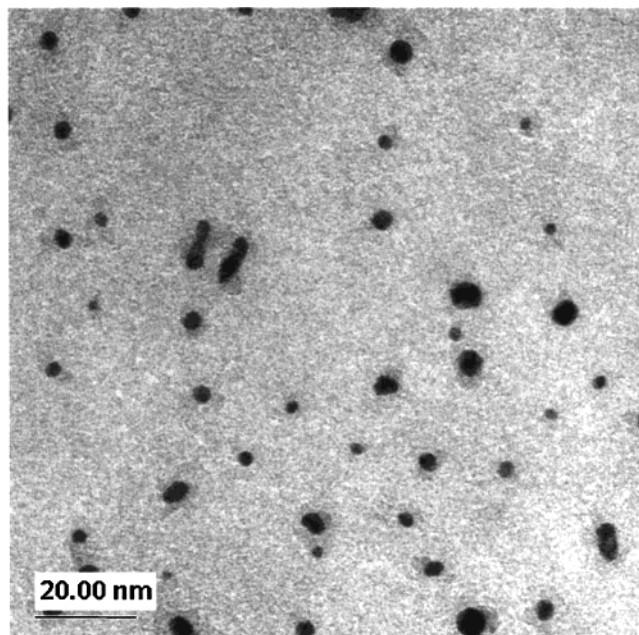


**Figure 5.** TEM micrograph of a sample prepared 2 min after all of the  $\text{Na}_2\text{S}$  was added following Method C.

**Method B.** The procedure was the same as in method A with the exception that  $\text{Na}_2\text{S}$  was added with no time interval.

**Method C.** The procedure was the same as in method A with the exception that the  $\text{HAuCl}_4$  solution was purged with argon gas for 30 min prior to mixing with  $\text{Na}_2\text{S}$ .

**Method D.** The procedure was the same as in method A with the exception that both the  $\text{Na}_2\text{S}$  and  $\text{HAuCl}_4$  solution were purged for 30 min prior to mixing.

**Method E.** A 40 mL sample of Milli-Q water was purged for 10 min prior to the addition of 1 mL of 0.02M  $\text{HAuCl}_4$ . To this 60  $\mu\text{L}$  of 0.1M  $\text{Na}_2\text{S}$  was added. After a period of 5 min, 20  $\mu\text{L}$  of  $\text{Na}_2\text{S}$  solution was added.

**Method F.** Gold nanoparticles not involving the use of sulfur were prepared from a classic recipe:<sup>23</sup> 95 mL of  $\text{HAuCl}_4$  solution containing 2.5 mg Au was heated to boil. To this boiling solution was added 10 mL of 1% sodium citrate solution. In a period of 5–10 min the solution color turned from white to grayish pink to brilliant wine red. Stable colloidal gold solutions were formed with fairly monodisperse gold nanoparticles with an average particle diameter of 15 nm. The solutions are indefinitely stable as long as no contamination is present. To prepare the gold aggregates, very small amounts of pyridine, or of sodium chloride, or of cationic surfactant (cetyltrimethylammonium chloride CTAC) were added to the gold solution.<sup>24,25</sup> The color of the solution was immediately changed to grayish pink or dark blue depending on the degree of aggregation. In general, the addition of a large amount of pyridine, or sodium chloride, or surfactant caused the gold particles to change color, and aggregate faster.

Transmission electron microscopy (TEM) and electron energy loss Spectroscopy (EELS) data were collected at the National Center for Electron Microscopy at Lawrence Berkeley Laboratory. The EELS data were collected at the S and Au edges to generate elemental maps of the sample. Energy Dispersive X-ray (EDX) analysis was also done to determine sample composition. The TEM samples were prepared from the reaction solution at the early stages of the reaction and over an hour after the reaction. The particles were also stable in the electron beam.

X-ray absorption data were taken at the Stanford Synchrotron Radiation Laboratory using beam line 4.3. Four XAFS samples

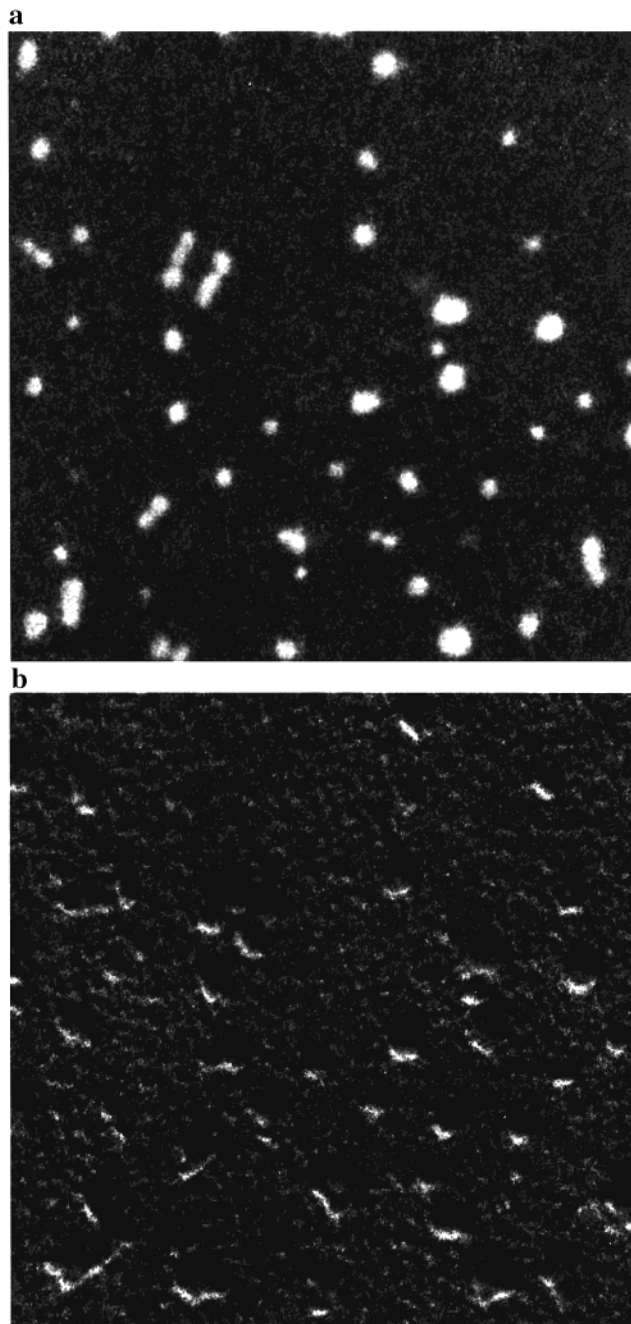


**Figure 6.** (a) Elemental map of Gold compiled from Au EELS data from a sample prepared 2 min after all  $\text{Na}_2\text{S}$  was added following method C. (b) Elemental map of Sulfur compiled from S EELS data from a sample prepared 2 min after all  $\text{Na}_2\text{S}$  was added following method C.

were prepared. One sample consisted of Au nanoparticles, prepared by method F, adsorbed onto filter paper. The others consisted of  $\text{HAuCl}_4$ – $\text{Na}_2\text{S}$  reaction solution, one prepared by method C with a 2 h reaction time, and the other two were prepared by method E with 15 and 45 min reaction times, respectively. The sample prepared by method C was stabilized with PVA. All three XAFS samples were absorbed on filter paper. Fluorescence data were taken at the Au  $L_3$  edge at 20 K. The fluorescence data were reduced by fitting the pre and postedge backgrounds to a straight line and a spline respectively.<sup>26,27</sup> The XAFS were then Fourier transformed and fitted in real space using RSFIT<sup>26,27</sup> with standards generated by FEFF7.<sup>28</sup> An  $\text{Au}_2\text{S}$  theoretical standard, based on the cuprite structure, was also generated using FEFF7.

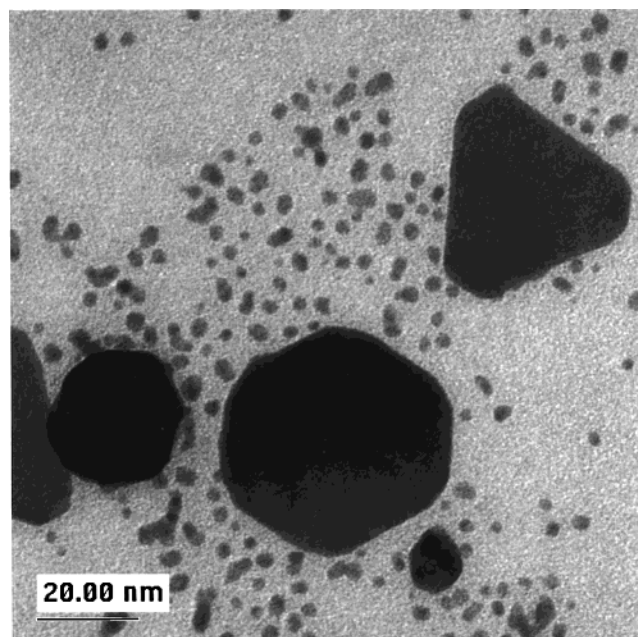


**Figure 7.** TEM micrograph of a sample prepared 2 h after all of the  $\text{Na}_2\text{S}$  was added following method C.

## Results

Methods A, B, C, and E generate similar UV-vis spectrum (Figure 1), but method E is the easiest to reproduce. After approximately 1 h the transverse and longitudinal plasma resonances can be clearly seen at  $\sim 525$  and  $\sim 920$  nm, respectively. Ten minutes latter both plasma resonances blue shifted. The transverse plasmon shifted to approximately  $\sim 520$  nm, and the longitudinal plasmon shifted to approximately  $\sim 825$  nm. After 2 h the transverse plasmon remained at  $\sim 520$  nm while the longitudinal plasmon blue shifted further to  $\sim 720$  nm. Both resonances grew in intensity as the reaction progressed, but the transverse plasmon remained more intense than the longitudinal plasmon. Following method D the plasma resonances displayed slightly different dynamics. In Figure 2 the dynamics of this reaction are displayed. The transverse plasmon remained at  $\sim 532$  nm throughout the reaction, but grew in intensity as the reaction progressed. The longitudinal plasmon, however, shifted from  $\sim 915$  to  $\sim 834$  nm over a period of an hour. It became more intense than the transverse plasmon.

It is interesting to compare the results without the use of  $\text{Na}_2\text{S}$ . The UV spectrum of the gold particles prepared with sodium citrate was almost identical to that of the gold solutions prepared from methods A–E. When pyridine, sodium chloride, or a cationic surfactant was added, the particles began to aggregate and the solution began to turn blue. A new adsorption peak at about 800 nm appeared (Figure 3). During the aggregation process, the peak at 530 nm remained relatively unchanged; the broad peak at 800 nm became more intense, and gradually shifted to 850 nm. This trend is almost identical to what was observed in Figures 1 and 2. However, one needs to be reminded that the gold particle prepared from sodium citrate is a clean system in that first the particles were uniform in size, and second the particle size did not change when the optical spectra changed during aggregation. Most importantly no sulfide ions were needed to cause the change in the absorption spectrum.

The TEM data in general show that methods A–E produce particles with a large particle distribution (Figure 4) with smaller particles ( $\sim 5$  nm) being predominant. There were also a variety of particle shapes. Spheroidal particles dominated, but there were

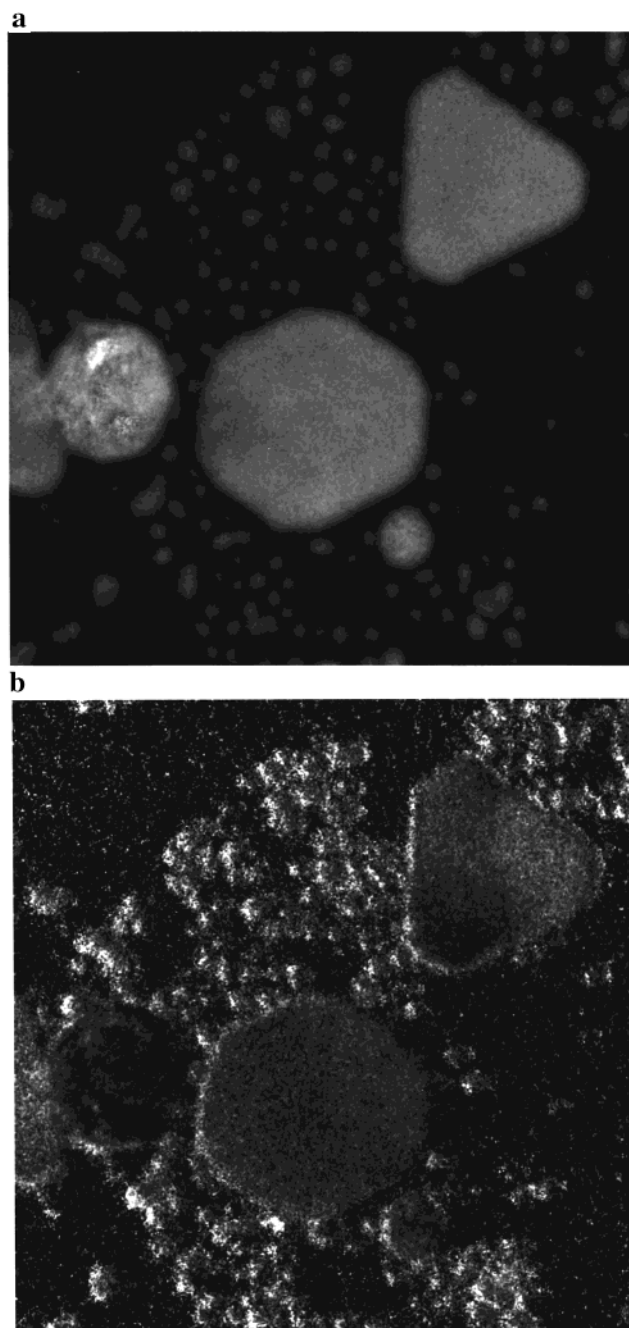


**Figure 8.** (a) Elemental map of Gold compiled from Au EELS data from a sample prepared 2 h after all  $\text{Na}_2\text{S}$  was added following method C. (b) Elemental map of Sulfur compiled from S EELS data from a sample prepared 2 h after all  $\text{Na}_2\text{S}$  was added following method C.

**TABLE 1: The Measured XAFS Parameters for the Gold Nanoparticles and  $\text{HAuCl}_4$ – $\text{Na}_2\text{S}$  Reactions**

parameters	15 min	45 min	2 h	Au nanoparticles
Au–Au distance ( $\text{\AA}$ )	2.878	2.879	2.867	2.868
Au–Au coordination number	7	7	12	12
Au–S distance ( $\text{\AA}$ )	2.314	2.317		
Au–S coordination number	0.7	0.7		

some rod and other shaped particles. Also the micrographs showed a similar pattern regardless of the reaction conditions. The composition of the particles, large and small, is primarily gold, with trace amount of sulfur as determined by energy dispersive spectroscopy (EDS). The particles display the lattice planes characteristic of gold. More importantly, the high-resolution TEM images revealed that many gold particles were

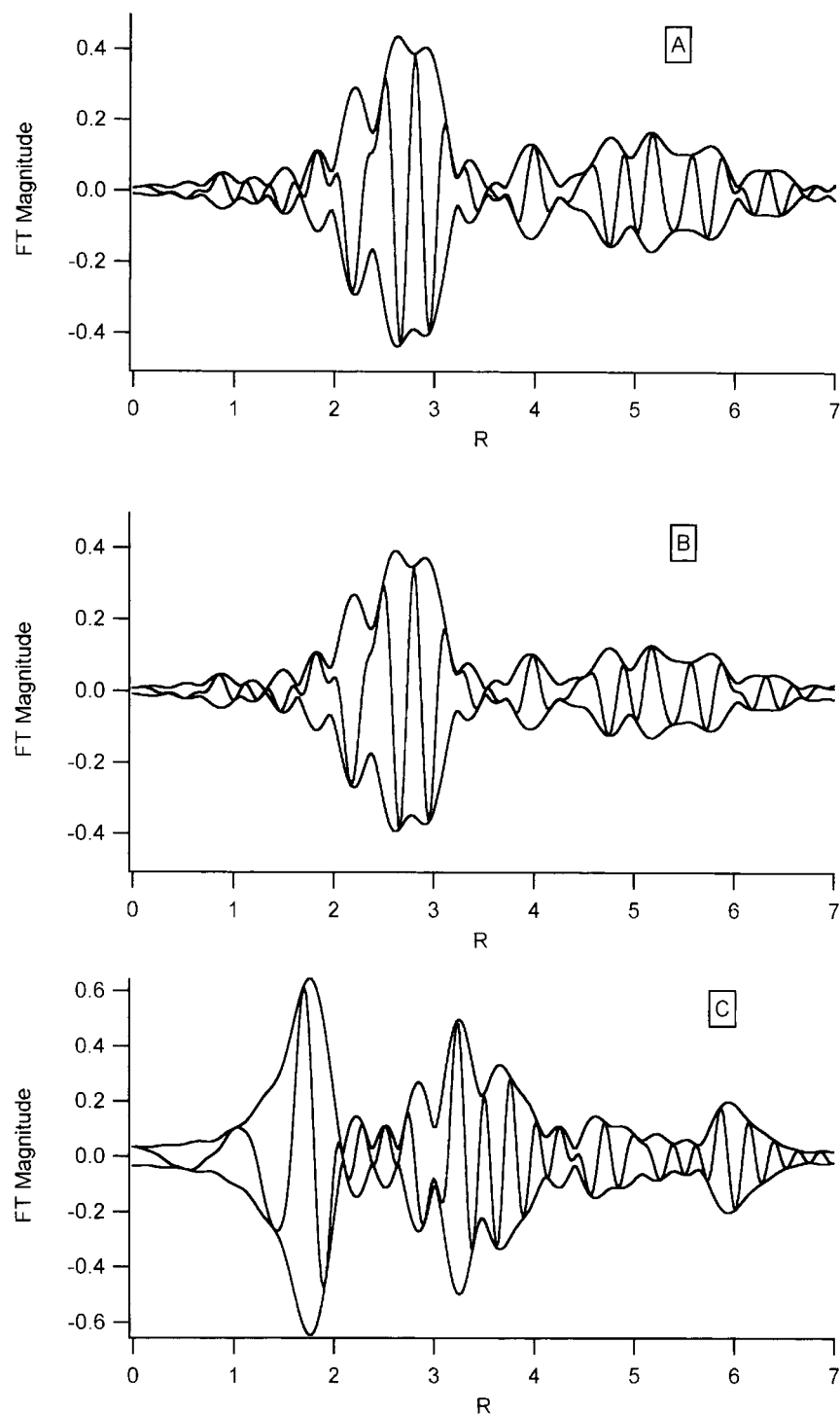


**Figure 9.** FT-XAFS of (A) Au nanoparticles, (B) HAuCl<sub>4</sub>-Na<sub>2</sub>S reaction solution after 2 h, and a (C) theoretical FT-XAFS plot of Au<sub>2</sub>S possessing the cuprite structure. The units of  $R$  are angstrom, and  $R$  includes the XAFS phase shift. The Fourier transform range was 3–14  $k$ .

not completely separated from one. In many regions the lattice structures were continuous from one particle to another, a good indication of aggregates coexisting with dispersed particles in the sample (Figure 10). On the basis of previous work,<sup>25</sup> we believe that these aggregates were present in the solution. The existence of aggregates in solution was also corroborated by the color of the solution. Completely dispersed colloidal gold should have a wine red color.

The TEM micrographs prepared from the reaction solution of method C 2 min after all of the Na<sub>2</sub>S was added (Figure 5) indicate the existence of primarily smaller particles on the order

of ~5 nm. Energy filtered images using electron energy loss (EELS) technique were obtained from isolated particles to identify the spatial distribution of Au and S (Figure 6a,b). They revealed that sulfur was distributed on the outer surface of the gold particles, and that there was not much sulfur present in the system. After an hour gold nanoparticles on the order of 40 nm had formed (Figure 7), and they were surrounded by smaller particles ~5 nm. The gold regions had coalesced but remained imbedded in larger sulfur regions (Figure 8a,b). In summary, it is safe to conclude that the TEM and energy filtered images did not provide any direct evidence of Au<sub>2</sub>S/Au core/shell

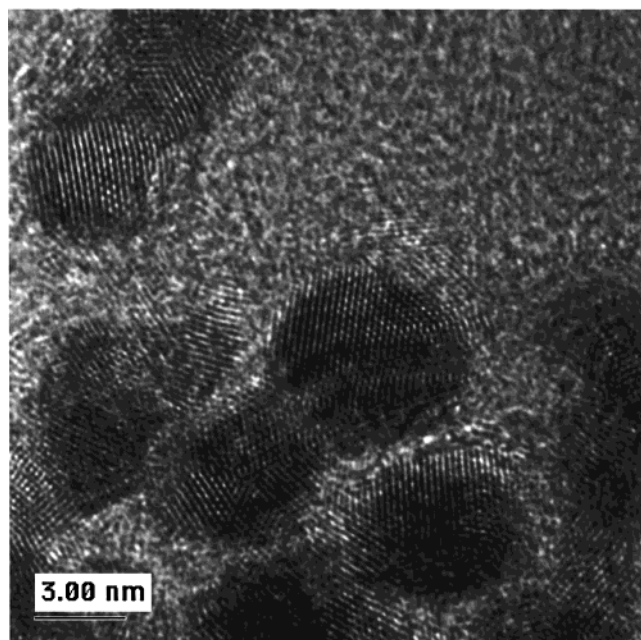


**Figure 10.** HRTEM micrograph of a sample prepared 2 h after all of the  $\text{Na}_2\text{S}$  was added following method C. The lattice planes are consistent with that of Au.

structure. On the contrary, it seems that S most likely precipitated around the gold particles as amorphous material and clusters.

The XAFS data also strongly refutes the presence of an  $\text{Au}_2\text{S}/\text{Au}$  core/shell structure (Table 1). XAFS acts as a probe of the local environment around the absorbing atom. Atoms with different local environments will have different XAFS, and atoms of the same or similar local environments will have similar XAFS. The XAFS of the 2-h  $\text{HAuCl}_4\text{-Na}_2\text{S}$  reaction solution was virtually identical to that of the XAFS of gold nanoparticles and showed no resemblance to the calculated  $\text{Au}_2\text{S}$  XAFS (Figure 9). However, these XAFS will be dominated by the larger particles since most of the gold atoms are in these large particles. The interatomic distance of the first coordination shell for the Au nanoparticles and the 2-h reaction solution were identical to each other and similar to bulk gold,<sup>29</sup> being 2.868 and 2.867 Å, respectively. The XAFS of the reaction solution also showed no evidence of direct gold–sulfur coordination, as mandated by the  $\text{Au}_2\text{S}/\text{Au}$  core/shell structure. One would expect gold sulfur coordination to occur at  $\sim 1.8$  Å,<sup>30</sup> which is the position of the first shell in  $\text{Au}_2\text{S}$  (Figure 9c). These data suggest that at the 2-h point the large particles are gold nanoparticles. HRTEM pictures of the smaller particle in the same time frame (Figure 10) indicate the small particles are gold nanoparticles. The XAFS from the 15- and 45-min reaction time frame should have more contribution from the smaller particles since the TEM data suggests that there are few large particles in the early time frame. When the XAFS from all three time frames are compared (Figure 11), some minor differences can be seen, suggesting that gold nanoparticles and another substance form early in the reaction. The XAFS for the 15- and 45-min samples can be fitted to the same gold standard used for the 2-h sample but with an Au–S coordination shell. The interatomic distance of the first coordination shell for the 15- and 45-min sample are 2.878 and 2.879 Å, respectively. These distances are slightly longer than that of those measured for the gold nanoparticles and the 2-h reaction, but the values are consistent with that of bulk gold. Further the coordination number for the first gold shell in the two samples was less than

that of the 2-h sample indicating that the two samples contain smaller particles.<sup>29</sup> The coordination number for the Au–S shell in the 15- and 45-min sample was less than one, suggesting that an S coordination was not a significant coordination for Au in these samples. Yet, the small S coordination is consistent with the idea of amorphous S on the surface of the particles. Since approximately 20% of the Au atoms in the particle are on the surface, one would expect to see a small signal from any surface species. The distance between the surface S and the Au is similar to the Au–S distance in Au–thiols,<sup>30</sup> but longer than that of  $\text{Au}_2\text{S}$  crystals.<sup>31</sup>

## Discussion

Three possible explanations for the near-infrared absorbance observed in Figures 1–5 are gold nanorods,  $\text{Au}_2\text{S}/\text{Au}$  (core/shell) particles, and gold nanoparticle aggregates. Since these particle systems produce similar, if not identical, optical absorbance spectrum, other analytical techniques are needed to determine definitively which is responsible for the observed near-IR absorbance. Here we conducted XAFS, and electron microscopy data analysis on the nanoparticles formed by the reduction of  $\text{HAuCl}_4$  with  $\text{Na}_2\text{S}$ . Our results strongly suggest that it was gold nanoparticle aggregates that produced the optical absorbance spectrum instead of nanoshells or nanorods.

The gold absorbance in the near-infrared is due to the optical resonance of the longitudinal dipole polarization of the electronic vibrations. Normally this resonance would coincide with the transverse resonance, which appears in the visible. Qualitatively, a shifted near-infrared peak indicates a change in the geometry of the particle because spherical gold nanoparticles poses only one resonance due to transverse and longitudinal plasma modes.<sup>4</sup> The change in position of the longitudinal plasmon with time also indicates that the sample was changing with time. The TEM results presented in Figures 6–8 excluded the formation of  $\text{Au}_2\text{S}/\text{Au}$  core shell structures over time, and suggest the gold nanoparticles were aggregating over time, and the aggregation caused the shift in the longitudinal plasma resonance. The observation of amorphous sulfur around the outer surface of gold is in direct contradiction to the previously proposed  $\text{Au}_2\text{S}/\text{Au}$  core/shell model, as is the lack of a strong Au–S peak in the XAFS data expected from an  $\text{Au}_2\text{S}$  core. Furthermore, we can exclude the rodlike structures because few were seen in direct TEM observations.

We suggest that the most likely origin of the near-infrared absorption is aggregation of gold nanoparticles. This is consistent with the spectra obtained from the gold aggregates prepared without any sulfur, in which the gold particles were spherical (not rodlike) and uniform in size, and these particles did not change their size during aggregation. The 15-nm gold particles were stabilized by the adsorbed citrate ions, which gave a negative charge to the particle surface. The repulsive forces from the negative charge kept the particles suspended and stable. The addition of pyridine displaced the citrate ions on the particle surfaces, and caused the particles to aggregate. Sodium chloride also caused aggregation because of the screening effect of the electrolyte ions. Cationic surfactant caused aggregation by neutralizing the negative charge on the surface. Previous studies suggested that once the particles were aggregated, hard agglomerates formed and the particles became fused together, similar to what is revealed in Figure 7.<sup>23–25</sup> Recent small-angle X-ray scattering data on gold particles produced by reduction of  $\text{HAuCl}_4$  with  $\text{Na}_2\text{S}$  also show clear evidence of aggregates.<sup>32</sup>

By examining the reduction reaction in detail, the nature of the product may be revealed. The reducing agent in the reaction

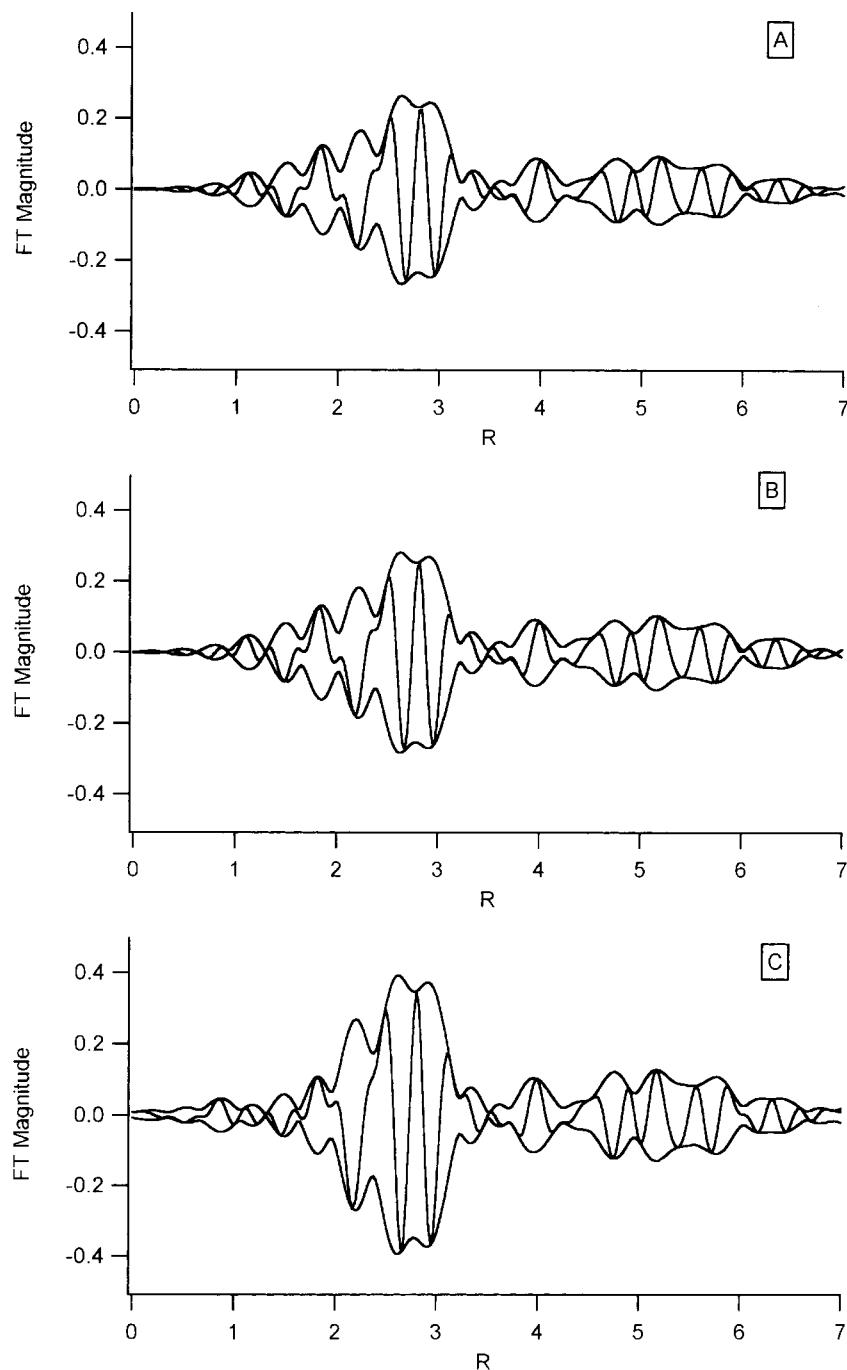
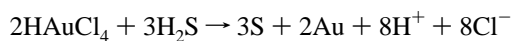


**Figure 11.** FT-XAFS of (A)  $\text{HAuCl}_4\text{-Na}_2\text{S}$  reaction solution after 15 min, (B)  $\text{HAuCl}_4\text{-Na}_2\text{S}$  reaction solution after 45 min, and (C)  $\text{HAuCl}_4\text{-Na}_2\text{S}$  reaction solution after 2 h. The units of  $R$  are angstrom, and  $R$  includes the XAFS phase shift. The Fourier transform range was 3–14  $k$ .

of  $\text{HAuCl}_4$  with  $\text{Na}_2\text{S}$  is  $\text{S}^{2-}$ . This species can take many forms in aqueous solutions depending upon the pH. At pH below 7, which was the conditions for our reaction,  $\text{S}^{2-}$  exists in solution primarily as  $\text{HS}^-$ .<sup>33</sup> The reaction pathway was most likely:



This pathway is supported by the drop in pH observed during the reaction. Gold(III) salts can react with  $\text{H}_2\text{S}$  to form  $\text{Au}_2\text{S}_3$ , but this reaction does not occur at room temperature or in aqueous solutions.<sup>33</sup> Also since elemental gold and sulfur are not likely to form a compound, gold nanoparticles should be the primary product of the reaction.<sup>34,35</sup>

Nanoparticles are stable in solution due to the electrostatics repulsion of their charged surface. Lack of sufficient surface

charge or stabilizing agent will cause the particles to aggregate or precipitate. Gold reduced by sodium citrate produces nanoparticles with citrate ions adsorbed onto the particle's surface, creating a surface charge that stabilizes the particles.<sup>23</sup> As shown here and demonstrated by others, pyridine can be used to disrupt the surface of citrate ions causing particle aggregation. In the reaction between  $\text{HAuCl}_4$  and  $\text{Na}_2\text{S}$  only Au nanoparticles and S are formed. Due to the presence of sulfur, sulfur defects on the surface of the particle should be present, and this is what was seen in our TEM data. Also the 5-nm blue shift in the transverse plasmon (Figure 1) could have been caused by the deposition of sulfur on the particle's surface. Since there are no species in solution to generate sufficient surface charge on the forming particles, the particles will aggregate. This aggregation should cause a red shift in the gold longitudinal plasma

resonance, and the lack of stability would cause the particles to precipitate from solution. Both of the phenomena were observed. It is interesting to note that when the reaction was conducted in the presence of PVP or some other polymer stabilizer the red shift in the longitudinal plasmon failed to occur.

### Conclusion

Another explanation for the evolution of the absorption spectrum of the reaction of HAuCl<sub>4</sub> with Na<sub>2</sub>S may be the formation of aggregates of Au nanoparticles as opposed to Au coated Au<sub>2</sub>S nanoparticles. The optical absorption spectrum is consistent with that seen in gold aggregates, and the Au XAFS data do not show any significant signs of sulfur neighbors present in the system. The electron microscopy data suggest that the aggregation process occurred by the coating of Au nanoparticles with S followed by the clustering of the coated particles.

**Acknowledgment.** We would like to thank Prof. Greg Szulczewski for initially bringing to our attention the possibility that core/shell structure may not be the correct explanation for the observed NIR absorption band and for many stimulating discussions afterward. We thank Alison Breeze for our helpful conversations. Also we would like to thank Chris Nelson, Chengyu Song, John Turner, and Christian Kisielowski at the National Center for Electron Microscopy for their assistance. This project was supported by grants from MBRS/NIH GM58903, GAANN, UC LEADS, the DOE at SSRL, the Petroleum Research Fund administered by the American Chemical Society, the Collaborative UC/Los Alamos National Labs (CULAR), the Materials Research Institute of Lawrence Livermore National Laboratories, and the California Energy Commission.

### References and Notes

- (1) Meriaudeau, F.; Downey, T.; Wig, A.; Passian, A.; Buncick, M.; Ferrell, T. L. *Sens. Actuators, B* **1999**, *54*, 106.
- (2) Mie, G. *Ann. Physik* **1908**, *25*, 377.
- (3) Kreibig, U.; Genzel, L. *Surf. Sci.* **1985**, *156*, 678.
- (4) Creighton, J. A.; Eadon, D. G. *Faraday Trans. J. Chem. Soc.* **1991**, *87*, 3881.
- (5) Link, S.; El-Sayed, M. *J. Phys. Chem. B* **1999**, *103*, 8410.
- (6) van der Zande, B.; Bohmer, M. R.; Fokkink, L. G. J.; Schonberger, C. *J. Phys. Chem. B* **1997**, *101*, 852.

- (7) van der Zande, B. M. I.; Koper, G. J. M.; Lekkerkerker, N. W. *J. Phys. Chem. B* **1999**, *103*, 5754.
- (8) van der Zande, B. M. I.; Pages, L.; Hikmet, R. A. M.; van Blaaderen, A. *J. Phys. Chem. B* **1999**, 5761.
- (9) Link, S.; Mohamed, M. B.; El-Sayed, M. A. *J. Phys. Chem. B* **1999**, *103*, 3073.
- (10) Yu, Y.; Chang, S.; Lee, C.; Wang, C. R. *J. Phys. Chem. B* **1997**, *101*, 6661.
- (11) Shipway, A. N.; Lahav, M.; Gabai, R.; Willner, I. *Langmuir* **2000**, *16*, 8789.
- (12) Dimon, P.; Sinha, S. K.; Weitz, D. A.; Safinya, C. R.; Smith, G. S.; Varady, W. A.; Lindsay, H. M. *Phys. Rev. Lett.* **1986**, *57*, 595.
- (13) Shih, W. Y.; Liu, J.; Shih, W. H.; Aksay, I. A. *J. Stat. Phys.* **1991**, *62*, 961.
- (14) Mayya, K. S.; Patil, V.; Sastry, M. *Bull. Chem. Soc. Jpn.* **2000**, *73*, 1757.
- (15) Lazarides, A. A.; Schatz, G. C. *J. Phys. Chem. B* **2000**, *104*, 460.
- (16) Blatchford, C. G.; Campbell, J. R.; Creighton, J. A. *Surf. Sci.* **1982**, *120*, 435.
- (17) Wilcoxon, J. P.; Martin, J. E.; Schaefer, D. W. *Phys. Rev. A* **1989**, *39*, 2675.
- (18) Zhou, H. S.; Honma, I.; Komiyama, H.; Haus, J. W. *Phys. Rev. B* **1994**, *50*, 12052.
- (19) Barnickel, P.; Wokaun, A. *Mol. Phys.* **1989**, *67*, 1355.
- (20) Averitt, D.; Sarkar, D.; Halas, N. J. *Phys. Rev. Lett.* **1997**, *78*, 4217.
- (21) Oldenburg, S. J.; Averitt, R. D.; Westcott, S. L.; Halas, N. J. *Chem. Phys. Lett.* **1998**, *288*, 243.
- (22) Szulczewski, G. 2000. Personal communication.
- (23) J Turkevich, P. L.; Stevenson, J.; Hillier, J. *Discuss. Faraday Soc* **1951**, *11*, 55.
- (24) Weitz, D. A.; Olivera, M. *Phys. Rev. Lett* **1984**, *52*, 1433.
- (25) Liu, J.; Shih, W. Y.; Sarikaya, M.; Aksay, I. A. *Phys. Rev. A* **1990**, *41* (4), 3206–13.
- (26) Li, G. G.; Bridges, F.; Booth, C. H. *Phys. Rev. B* **1995**, *52*, 6332.
- (27) Bridges, F.; Booth, C. H.; Li, G. G. *Phys. B* **1995**, *208–209*, 121.
- (28) Zabinsky, S. I.; Rehr, J. J.; Ankudinov, A.; Albers, R. C.; Eller, M. J. *Phys. Rev. B* **1995**, *52*, 2995.
- (29) Fairbanks, M. C.; Benfields, R. E.; Newport, R. J. *Solid State Commun.* **1990**, *73*, 431.
- (30) Zanchet, D.; Tolentino, H.; Martins Alves, H. C.; Alves, O. L.; Ugarte, D. *Chem. Phys. Lett.* **2000**, *323*, 167.
- (31) Ishikawa, K.; Isonaga, T.; Wakita, S.; Suzuki, Y. *Solid State Ionics* **1995**, *79*, 60.
- (32) Norman, T.; Grant, C.; Magana, D.; Zhang, J.; Cao, D.; Bridges, F.; Liu, J.; van Buuren, T. *SPIE Proc.* 2002. Submitted for publication.
- (33) Pourbaix, M. *Atlas of Electrochemical Equilibria in Aqueous Solutions*; 2nd English ed.; National Association of Corrosion Engineers: Houston, 1974.
- (34) Puddephatt, R. J. *The Chemistry of Gold*; Elsevier: Amsterdam, 1978; Chapter 2.
- (35) Morris, T.; Copeland, H.; Szulczewski, G. *Langmuir* **2002**, *18*, 535.